Methanol Desorption from Cu-ZSM-5 Studied by In Situ Infrared Spectroscopy and First-Principles Calculations

Xueting Wang,[†] Adam A. Arvidsson,[‡] Magdalena O. Cichocka,[¶] Xiaodong Zou,[¶] Natalia M. Martin,[†] Johan Nilsson,[†] Stefan Carlson,[§] Johan Gustafson,[‖] Magnus Skoglundh,[†] Anders Hellman,[‡] and Per-Anders Carlsson[*,†]

†*Department of Chemistry and Chemical Engineering and Competence Centre for Catalysis, Chalmers University of Technology, Gothenburg, 412 96, Sweden*

‡*Department of Physics and Competence Centre for Catalysis, Chalmers University of Technology, Gothenburg, 412 96, Sweden*

¶*Berzelii Center EXSELENT on Porous Materials, Department of Materials and Environmental Chemistry, Stockholm University, 106 91 Stockholm, Sweden*

§*MAX-IV Laboratory, Lund University, Lund, 221 00, Sweden*

‖*Synchrotron Radiation Research, Lund University, Lund, 221 00, Sweden*

E-mail: per-anders.carlsson@chalmers.se

Abstract

The dynamic interaction of methanol and its derivatives with Cu-exchanged ZSM-5 during methanol temperature programmed desorption from 30 to 450 °C has been investigated using *in situ* diffuse reflectance infrared Fourier transform spectroscopy and first-principles calculations. The results emphasize that defects in the framework structure of the zeolite and Brønsted acid sites constitute ion-exchange sites for Cu

ions. The Cu sites introduced in ZSM-5 actively interact with methanol adsorbed at moderate temperature, *i.e.* below 250 °C, and take roles in further oxidation of the adsorbed species to formate and CO. Moreover, spectra recorded at higher temperatures, *i.e.* above 300 °C, after adsorption of methanol show strong interaction between methoxy groups and the zeolite framework, suggesting that under mild conditions proton extraction for methanol production during direct partial oxidation of methane to methanol over Cu-ZSM-5 is necessary.

Introduction

Conversion of methane to methanol in a one-step oxidation process is an attractive route for methanol synthesis as well as for converting natural gas and biogas into more easily transported feedstock or fuel. A main challenge is how to activate methane (and oxygen) for subsequent partial oxidation to methanol without opening up for unwanted over-oxidation to, *i.e.* carbon monoxide, carbon dioxide, formate and water. It has been recognized that mild reaction conditions and the use of catalysts are necessary ingredients,[1] although yet the appropriate catalyst formulation for industrial methanol production is unknown. Inspired by nature, and in particular the enzyme methane monooxygenases (MMO) that selectively can oxidize methane to methanol at ambient conditions,[2–4] metal-functionalized zeolites have been proposed to be promising inorganic counterparts to facilitate this reaction when molecular oxygen (O_2) is used as oxidant for methane under mild conditions. Zeolites are aluminosilicates with well-defined micropororus structures that can accommodate various small metal species. When functionalized with Cu they resemble the active dicopper centers in MMOs, which are proposed to be responsible for methane oxidation to methanol.[5,6] The focus of recent studies has, on the one hand, been to identify the active site for the reaction and, on the other hand, to complete a true catalytic cycle. In both cases the aim has been to improve the catalysts and/or the catalytic process.

By use of Raman spectroscopy and density functional theory (DFT) calculations, the

active site for direct partial oxidation of methane to methanol in Cu-ZSM-5 has been assigned to a bent mono-(μ-oxo)dicupric species.[7] The presence of this site has been reported to correlate with an absorption band at 22700 cm^{-1} in the UV-visible spectrum,[8,9] which then has been used as an indicator of the active site when characterizing Cu-ZSM-5[10,11] and Cu-MOR.[12] There are, however, recent reports on Cu-exchanged zeolites that possess catalytic activity for methane oxidation to methanol without showing the mentioned UV-vis band.[13,14] This suggests that the mono-(μ-oxo)dicupric cores may not be the sole active site and/or that the band assignment is not conclusive. As to the catalytic cycle, highly reactive Cu centres have traditionally been formed by oxidation of the catalyst at elevated temperatures (Activation), while to obtain methanol as a product, the activated catalyst is then exposed to methane (Reaction) in a second step before methanol can be formed by proton extraction of adsorbed methoxy groups[9,10,13,15] using water, ethanol or other proton sources (Extraction) in a final step. The entire process involves changes in both temperature and feed composition and is thus not a true catalytic cycle. Recently, however, Narsimhan *et al.*[13] reported catalytic oxidation of methane to methanol with high selectivity and sustained activity over Cu-ZSM-5 during prolonged time (288 h). The observed reaction rates, however, are far from satisfactory. The product extracted during one oxidation cycle remains below 82 μmol methanol/g_{cat}[5,8–10,13,16] and the continuous conversion of methane is low, around 0.001 %.[13] Due to this low catalytic activity, it is neither straightforward to determine the kinetics nor the nature of the active sites and the governing mechanisms behind direct partial oxidation of methane to methanol. In fact, achieving industrially reasonable catalytic activity for partial oxidation of methane has always been the major challenge.

Despite many efforts[11,15,17–20] and some progress in this area, the process of partial oxidation of methane to methanol remains a great challenge in modern chemistry. One important question still unclear is how methanol interacts with the catalyst. For example the stability of the adsorbed methoxy groups is a barrier for the removal of the product and the proton extraction of the methoxy groups may result in blockage of the active sites. Investigation

of the interaction between methanol and Cu-exchanged zeolites could give insight on how catalysts should be designed as to circumvent the stoichiometric approach of Activation-Reaction-Extraction.

In the present study, we use methanol temperature programmed desorption (TPD) to explore the interaction between methanol and Cu-ZSM-5 that has been prepared by aqueous ion-exchange. In particular, we monitor the evolution of surface species as a function of temperature by *in situ* infrared spectroscopy. Complementary first-principles calculations are made to support the interpretation of the spectroscopic results. We show that defects in the framework structure of the zeolite and Brønsted acid sites constitute ion-exchange sites for Cu ions. The Cu species introduced during ion-exchange are responsible for additional adsorption of methanol compared to the parent zeolite. Moreover, oxidation of adsorbed methanol and methoxy groups occurs over the Cu species. The results also indicate strong interaction between methoxy groups and the zeolite framework, supporting the observation that proton extraction may be necessary when zeolitic structures are used as hosts for the active Cu species for direct partial oxidation of methane to methanol.

Experimental and theoretical methods

Catalyst preparation and *ex situ* characterization

The Cu-ZSM-5 sample was prepared using aqueous ion-exchange.[9] The ion-exchange was carried out by mixing an aqueous solution of $Cu(NO_3)_2$ (0.1 M, 100 ml/g zeolite) with H-ZSM-5 (Si/Al = 13.5, Akzo Nobel) at room temperature for 24 hours. The pH value of the solution was kept constant at around 4.5 by addition of ammonia when necessary. After ion-exchange the sample was filtered, washed with Milli-Q water (18 MΩ·cm) and finally dried at 120 °C in air overnight.

The crystal phases of the zeolite samples were determined by X-ray diffraction (XRD) using a Bruker XRD D8 Advance instrument with monochromatic $CuK_{\alpha 1}$ radiation scan-

ning 2θ from 20 to 60 ° (step size 0.029 °, dwell time 1 s). The nitrogen adsorption-desorption isotherms were measured by a Micromeritics Tristar 3000 instrument at 77 K. Before measurements, the powder samples were degased in N_2 at 220 °C for 2 hours.

The *ex situ* X-ray absorption spectroscopy (XAS) measurements were performed at beamline I811 at the MAX-IV Laboratory, Lund, Sweden. The XAS data at the Cu K-edge (8979 eV) was collected in fluorescence mode. The photon energy was calibrated using a Cu foil measured simultaneously with the sample. The X-ray absorption near edge structure (XANES) spectra were normalized using the Athena software.[21] The Fourier transformation of the spectra were performed on k^2-weighted extended X-ray absorption fine structure (EXAFS) oscillations in the range of 3-14 $Å^{-1}$.

Transmission electron microscopy (TEM) analysis was performed using a JEOL JEM 2100F electron microscope at 200 kV. The H-ZSM-5 and Cu-ZSM-5 samples for TEM studies were ground, dispersed in ethanol and then ultra-sonicated. A droplet of the suspension was transferred to a TEM grid covered by holey carbon film. Selected area electron diffraction (SAED) patterns of H-ZSM-5 and Cu-ZSM-5 were collected. A through-focus series containing 20 high-resolution electron microscopy (HRTEM) images were acquired with a defocus step of -53.3 Å on a Gatan Ultrascan 1000 camera. The structure projection was reconstructed from the 20 HRTEM images using the software QFocus.[22] Scanning transmission electron microscopy (STEM) imaging and energy dispersive spectroscopy (EDS) mapping were recorded for the Cu-ZSM-5 specimen using a molybdenum grid and a beryllium sample holder in order to avoid the contribution of an external copper signal. High-angle annular dark-field (HAADF) STEM images and EDS maps were collected using a spot site of 1.5 nm.

In situ diffuse reflectance infrared Fourier transform spectroscopy

The *in situ* infrared spectroscopic measurements were all made in diffuse reflectance mode, *i.e.* diffuse reflectance infrared Fourier transform spectroscopy (DRIFTS). For this a VER-

TEX 70 spectrometer (Bruker) equipped with a liquid nitrogen cooled mercury cadmium telluride detector with the band width 600-12000 cm^{-1}, a Praying Mantis^{TM} diffuse reflectance accessory and a high-temperature stainless steel reaction chamber (Harrick Scientific Products Inc.) was used. The spectra were measured between 900 and 4000 cm^{-1} with a spectral resolution of 1 cm^{-1}. The instrumental aperture was 3 to 6 mm wide with an eight times sensitivity gain. To facilitate high spectral quality over the studied temperature interval and to avoid unnecessary changes of the sample bed, a sieved fraction between 38 and 75 μm of the parent sample was used. About 85 μl sample was loaded into the reaction chamber.

The methanol-TPD experiments were carried out for both the Cu-ZSM-5 sample and its parent zeolite, H-ZSM-5. After pre-treatment of the samples with O_2 at 550 °C for one hour, a few droplets of methanol (99.8 %, Sigma-Aldrich) was added to the sample at 30 °C. The following TPD experiments were carried out under 100 ml/min flow of pure Ar or 2 % O_2 balanced with Ar with stepwise temperature increase from 30 to 450 °C (the temperature interval is 25 °C for spectra taken between 50 and 450 °C). Each spectrum was taken 10 minutes after the sample reached the target temperature. The backgrounds were recorded in pure Ar or 2 % O_2 in Ar accordingly at 30 °C after the sample pre-treatment.

First-principles calculations

For the first-principles calculations the Vienna Ab-inito simulation package (VASP)[23,24] was used, where the interaction between the valence electrons and the cores was described by the Projector-Augmented Wave (PAW) scheme.[25] The exchange-correlation was described using the optB86b-vdW functional,[26] which includes non-local correlation contributions. Initial relaxations were achieved using PBE.[27] The Kohn-Sham equations were expanded in plane-waves with a kinetic energy cut-off value of 480 eV. The Brillouin zone was sampled using the Γ-point only. Energies were converged when the difference between two subsequent self-consistent steps was less than 10^{-6} eV.

The copper dimer was modelled as the $[Cu\text{-}O\text{-}Cu]^{2+}$ motif previously found to be a

plausible candidate for an active site for partial oxidation of methane in Cu-ZSM-5.[7,28,29] Each of the two Cu atoms were placed on top of the Al sites placed in the most energetically favourable configuration,[28] in the crossing between the straight and the sinusoidal channels in the framework. The copper monomer was modelled by removing one of the Cu-Al pairs in the dimer site, the one that proved to be less stable by 0.13 eV with PBE. The experimentally determined unit cell for MFI[30] was used for all structures.

Structural relaxation and vibrational frequencies were calculated using the Atomic Simulation Environment (v 3.11.0)[31] and VASP. Geometries were relaxed according to the quasi-Newton algorithm until the maximum force was less then 0.05 eV/Å. The vibrational analysis used central differences to obtain the Hessian matrix with a displacement of 0.01 Å.

Vibrational frequencies were calculated for species on Cu monomer, Cu dimer (the [Cu-O-Cu]$^{2+}$ motif) and Brønsted acid sites (Al + H^+), and on bare silicalite (MFI with no Al). These are presented in Table 1. More specifically we consider methanol (CH_3OH), methoxy (OCH_3), Brønsted acid site (Al-O-H), OH on the two copper sites, and carbonyl (Cu-CO) and formate (Cu-OCHO) on the copper monomer site. The methoxy on the Cu monomer site is also considered with an extra hydrogen that can donate one electron and reduce the formally Cu^{2+} to Cu^+.

Results and discussion

Sample characteristics

We start the discussion by commenting on the structural properties of the samples before presenting the analysis of the methanol temperature programmed desorption. As shown in Figure 1a the XRD pattern for both the Cu-ZSM-5 sample and its parent H-ZSM-5 exhibit characteristic peaks of the ZSM-5 crystal structure[32] with similar intensity, suggesting well preserved crystal structure after ion-exchange. No additional peak can be observed in the Cu-ZSM-5 pattern indicating the absence of copper and/or copper oxide particles above

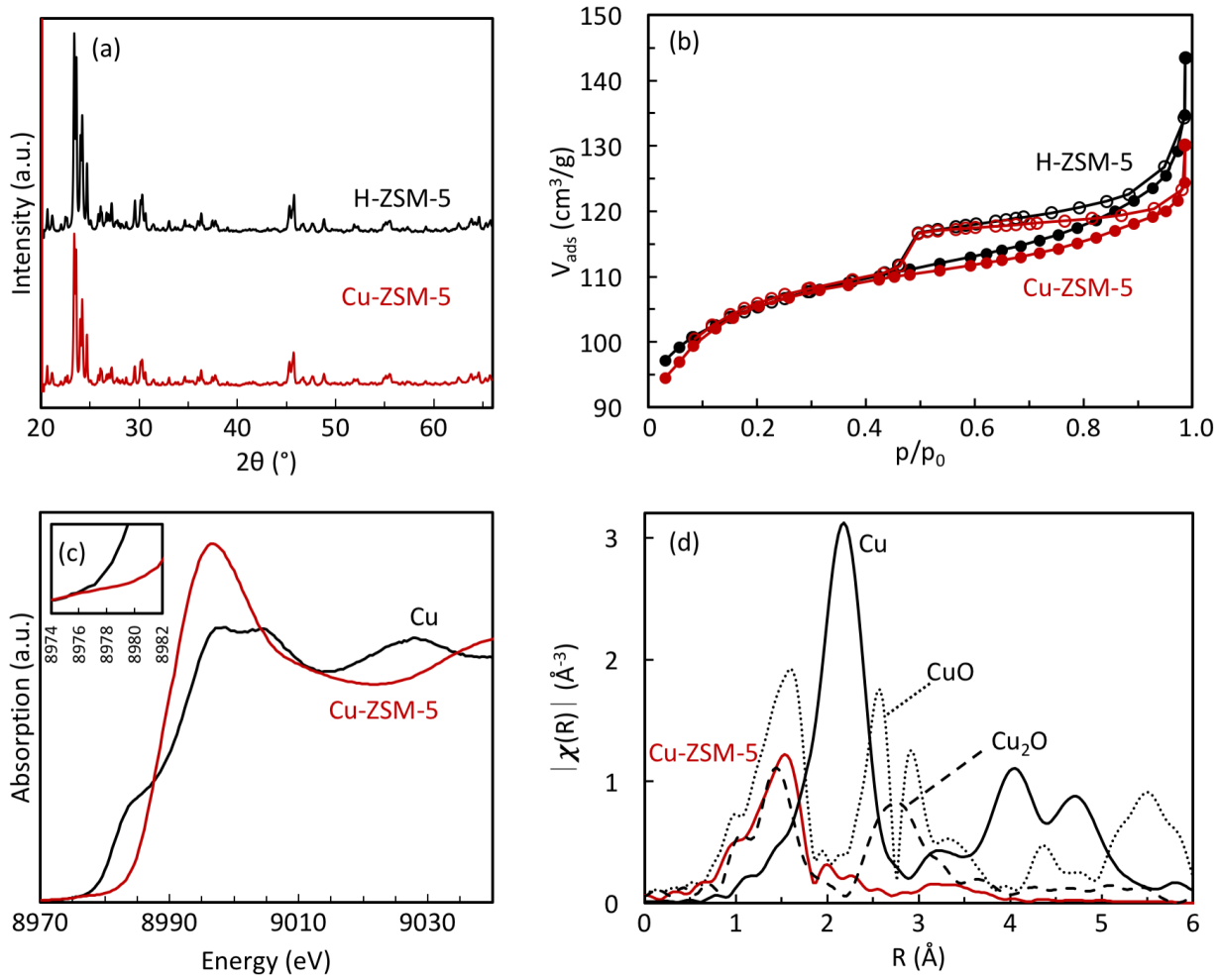

Figure 1: *Ex situ* characterization of the H-ZSM-5 and Cu-ZSM-5 samples. (a) XRD patterns of H-ZSM-5 (black) and Cu-ZSM-5 (red); (b) N_2 adsorption (closed symbols) and desorption (opened symbols) isotherms for H-ZSM-5 (black) and Cu-ZSM-5 (red); (c) XANES spectra of Cu-ZSM-5 (red) and Cu foil (black); (d) magnitude of Fourier transformed EXAFS spectra (k-weight = 2) of Cu-ZSM-5 (red), Cu foil (solid black line), Cu_2O (dashed black line, the Farrel Lytle database #cu2o.514) and CuO (dotted black line, the Farrel Lytle database #cuoxop.027).

2-3 nm in diameter. The N_2 adsorption-desorption isotherms for both the H-ZSM-5 and Cu-ZSM-5 samples are shown in Figure 1b. For the H-ZSM-5 sample, the t-plot calculation gives the specific surface area (SSA) of $357 \pm 9\,m^2/g$ and the micropore volume (V_{micro}) of $0.122\,cm^3/g$ (t-Range: 0.35-0.50 nm). The corresponding numbers for the Cu-ZSM-5 sample are $356 \pm 9\,m^2/g$ and $0.129\,cm^3/g$ (t-Range: 0.35-0.50 nm). The SSA and V_{micro} of both samples are reasonable for ZSM-5.[33,34] The N_2 adsorption-desorption isotherms for both samples are typical for the type IV isotherm with H4 hysteresis loops[35] closing at p/p_0 of about 0.4. This behavior is representative for ZSM-5 with low Si/Al ratio.[33,34] The hysteresis loops reflect the mesopores between aggregated zeolite crystals, cf. Figure S1 and S2. The high initial nitrogen uptake at p/p_0 below 0.1 can be associated with filling of micropores. The initial uptake is similar for both isotherms indicating similar accessible micropore volume in the Cu-ZSM-5 sample as in the parent H-ZSM-5. Therefore, the adsorption-desorption isotherms suggest well preserved pore structure of ZSM-5 after ion-exchange. The XANES spectrum for Cu-ZSM-5 in Figure 1c presents a sharp absorption at about 8995-8998 eV, which is due to the 1s to 4p electronic transition of Cu^{2+} species.[36] No obvious pre-edge feature for Cu^+ (well defined peak at 8982-8984 eV[36,37]) can be observed, indicating that the oxidation state of the Cu species is dominantly Cu^{2+}. The featureless pre-edge, however, eliminates the existence of CuO like structure (weak absorption at about 8976-8979 eV and shoulder at about 8985-8988 eV[37]). This indicates that the Cu-ZSM-5 sample does not contain detectable amounts of large CuO particles. The Fourier transforms of the Cu K-edge EXAFS spectra of the Cu-ZSM-5 sample and the reference compounds (the Farrel Lytle database[38]), *i.e.* Cu, Cu_2O and CuO, are presented in Figure 1d. The results obtained by curve fitting analysis of the EXAFS spectrum on the Cu-ZSM-5 sample is listed in the supplementary materials. The Cu-ZSM-5 sample exhibits a strong peak at around 1.5 Å (without phase shift correction) which is assigned to neighbouring O atoms (Cu-O). The lack of peaks in the range of 2.5-3 Å suggesting the absence of neighbouring Cu atoms (Cu-O-Cu), which indicates the presence of isolated Cu ions.

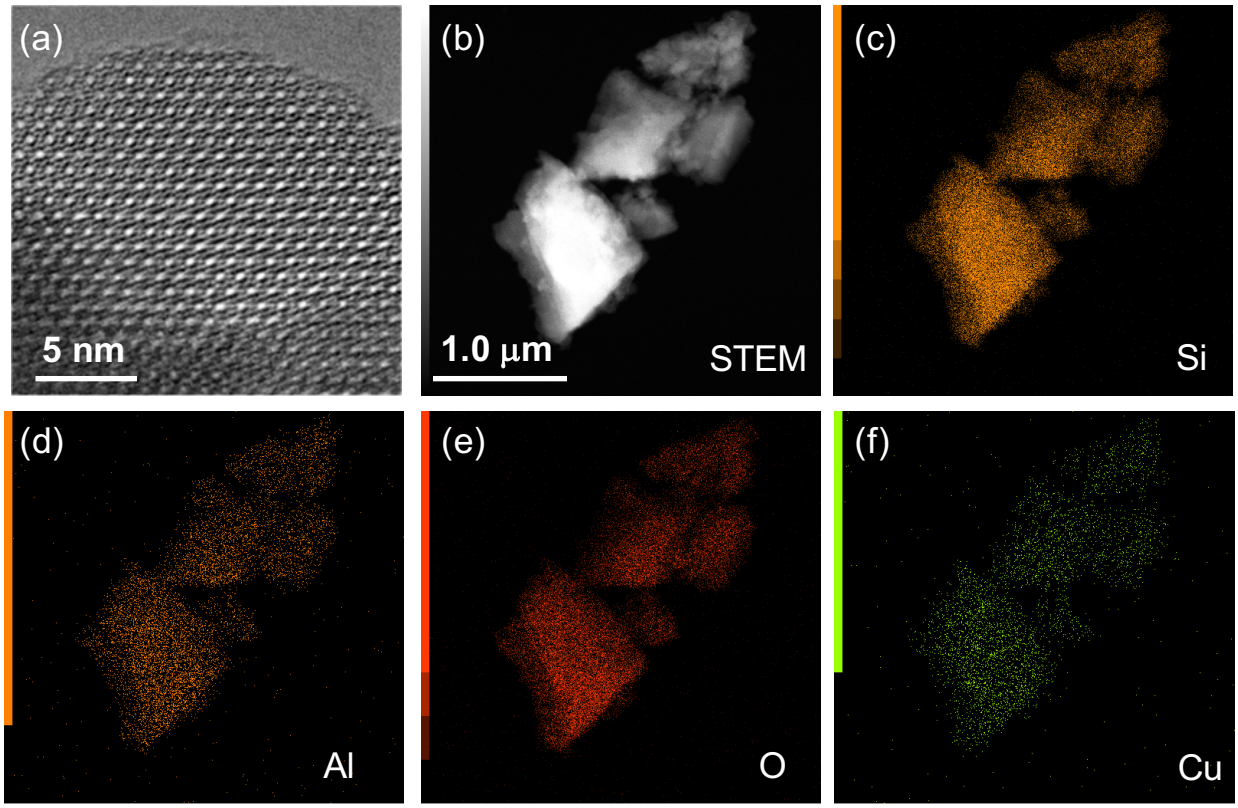

Figure 2: TEM characterization of the Cu-ZSM-5 sample. (a) Reconstructed structure projection from 20 HRTEM images taken along the b-axis showing the high crystallinity. (b) HAADF-STEM image showing the typical morphology of the Cu-ZSM-5 sample. (c-f) elemental maps of Si (c), Al (d), O (e) and Cu (f) obtained by EDS mapping showing the elemental distribution within the ZSM-5 crystals.

Figure 2 presents the TEM characterization of the Cu-ZSM-5 sample. The HRTEM image (Figure 2a) confirms that the high crystallinity of ZSM-5 remains after the ion-exchange with copper. The TEM analysis shows no significant changes in the morphology of the Cu-ZSM-5 particles (Figure S2) compared to that of the H-ZSM-5 particles (Figure S1). As observed from the STEM image and EDS maps (Figure 2b and f), Cu is distributed throughout the entire ZSM-5 crystals. No other extra copper were found in the Cu-ZSM-5 sample.

Infrared spectroscopy

For the spectroscopic results, we will focus the discussion on the vibrational regions that carry most of the spectroscopic information, namely, i) the O-H stretching region at 3300-4000 cm^{-1}, ii) the C-H stretching region at 2600-3100 cm^{-1} and iii) the C=O stretching/O-H bending region at 1500-2300 cm^{-1}. Each region is presented in Figure 3, 4 and 5, respectively. Table 1 summarizes the assignments and notations of the vibrational bands observed during the methanol-TPD experiments as well as those obtained from calculations for the Cu-ZSM-5 sample and its parent zeolite H-ZSM-5. We point out that the methanol-TPD experiment is reproducible and even so for an experiment with another Cu-ZSM-5 sample with different ion-exchange time (6 h). As an example, the IR spectra presented in Figure S9 in the SI are qualitatively similar to the ones for Cu-ZSM-5 with 24 h ion-exchange time, which will be discussed in detail hereunder.

After methanol adsorption, broad IR absorption bands appear in the region at 3800-2200 cm^{-1}, as shown in Figure S7. These bands represent OH containing species present in the zeolite after methanol adsorption: silanols interacting with methanol molecules via H-bonding, OH groups of hydrated copper ions and liquid-like methanol, i.e., methanol-methanol interactions. The intensity of these decrease as the temperature is increased due to the desorption and dehydration of methanol. The negative absorption peaks shown in the O-H stretching region (Figure 3) after methanol adsorption are due to the interaction of adsorbed methanol with OH groups on the framework structure of the zeolite. Two distinct

Table 1: First-principles calculation results and literature assignments of vibrational bands observed by DRIFTS for the Cu-ZSM-5 sample and its parent zeolite H-ZSM-5 during desorption of methanol.

Vibration	**Notation**	**Wavenumber (cm^{-1})**	**Motif[b]**	**Ref.**
O-H stretching region		**3300-4000**		
Isolated silanol	$\nu[Si-OH]_{iso}$	3745, 3618[a]	S10a	39–45
Isolated silanol on defect Si	$\nu[Si_{def}-OH]_{iso}$	3725		40,45
Isolated hydroxyl on isolated framework Al	$\nu[Al_{fr}-OH]_{iso}$	3781		44,46–48
Isolated hydroxyl on extra framework Al	$\nu[Al_{ex}-OH]_{iso}$	3668		42–44,49
Brønsted acid site (BAS)	$\nu[Si-O(H)-Al]$	3620, 3103[a]	S10b	41–43,49
Cu^+ monomer	$\nu[Cu^+-OH]$	3632[a]	S10c	
Cu^+ monomer	$\nu[Cu^+-O(H)(CH_3)]$	3761[a]	S12b	
Cu^+ dimer	$\nu[Cu^+-O(H)-Cu^+]$	3580[a]	S10d	
Cu^+ dimer	$\nu[Cu^+-O(H)(CH_3)-Cu^+]$	3413[a]	S12c	
C-H stretching region		**2600-3100**		
Methoxy on extra framework Si (asym)	$\nu_{as}[Si_{ex}-OCH_3]$	2957		39,40,44
Methoxy on extra framework Si (sym)	$\nu_s[Si_{ex}-OCH_3]$	2854		39,40,44
Methoxy formed at extra framework Al (asym)	$\nu_{as}[Al_{ex}-OCH_3]$	2968		44,45
Methoxy formed at BAS (asym)	$\nu_{as}[Si-O(CH_3)-Al]$	2978, 3064[a], 3079[a]	S11a	39,40,45
Methoxy formed at BAS (sym)	$\nu_s[Si-O(CH_3)-Al]$	2867, 2968[a]	S11a	39,40,45
Cu^+ monomer	$\nu[Cu^+-O(H)(CH_3)]$	2942[a], 3024[a], 3148[a]	S12b	
Cu^+ monomer	$\nu[Cu^+-OCH_3]$	2792[a], 2829[a], 2882[a]	S11c	
Cu^{2+} monomer	$\nu[Cu^{2+}-OCH_3]$	2693[a], 2930[a], 2984[a]	S11d	
Cu^+ dimer	$\nu[Cu^+-O(H)(CH_3)-Cu^+]$	2971[a], 3080[a], 3095[a]	S12c	
Cu^+ dimer	$\nu[Cu^+-O(CH_3)-Cu^+]$	2903[a], 2987[a], 3016[a]	S11b	
DME hydrogen bonded to BAS	$\nu[BAS-O(CH_3)_2]$	2946, 3011		45
Methanol hydrogen bonded	$\nu[CH_3OH(liq)]$	2849, 2955, 3002		44,45
Methanol hydrogen bonded to BAS	$\nu[BAS-O(H)(CH_3)]$	2841, 2909[a], 2991[a], 3056[a]	S12a	50
A band of the (A, B, C) triplet		∼2780		51
C=O stretching / O-H bending region		**1500-2300**		
Carbonyl on Cu^+	$\nu[Cu^+-CO]$	2157, 2124[a]	S13a	52
C band of the (A, B, C) triplet		1742		51,53,54
Water	δ[HOH]	1647		39,55,56
Formate	$\nu[Cu^+-OCHO]$	1575, 1614[a]	S13b	40,57

[a]DFT assignments from this work

[b]Motifs listed in the supplementary materials Figure S10-S13

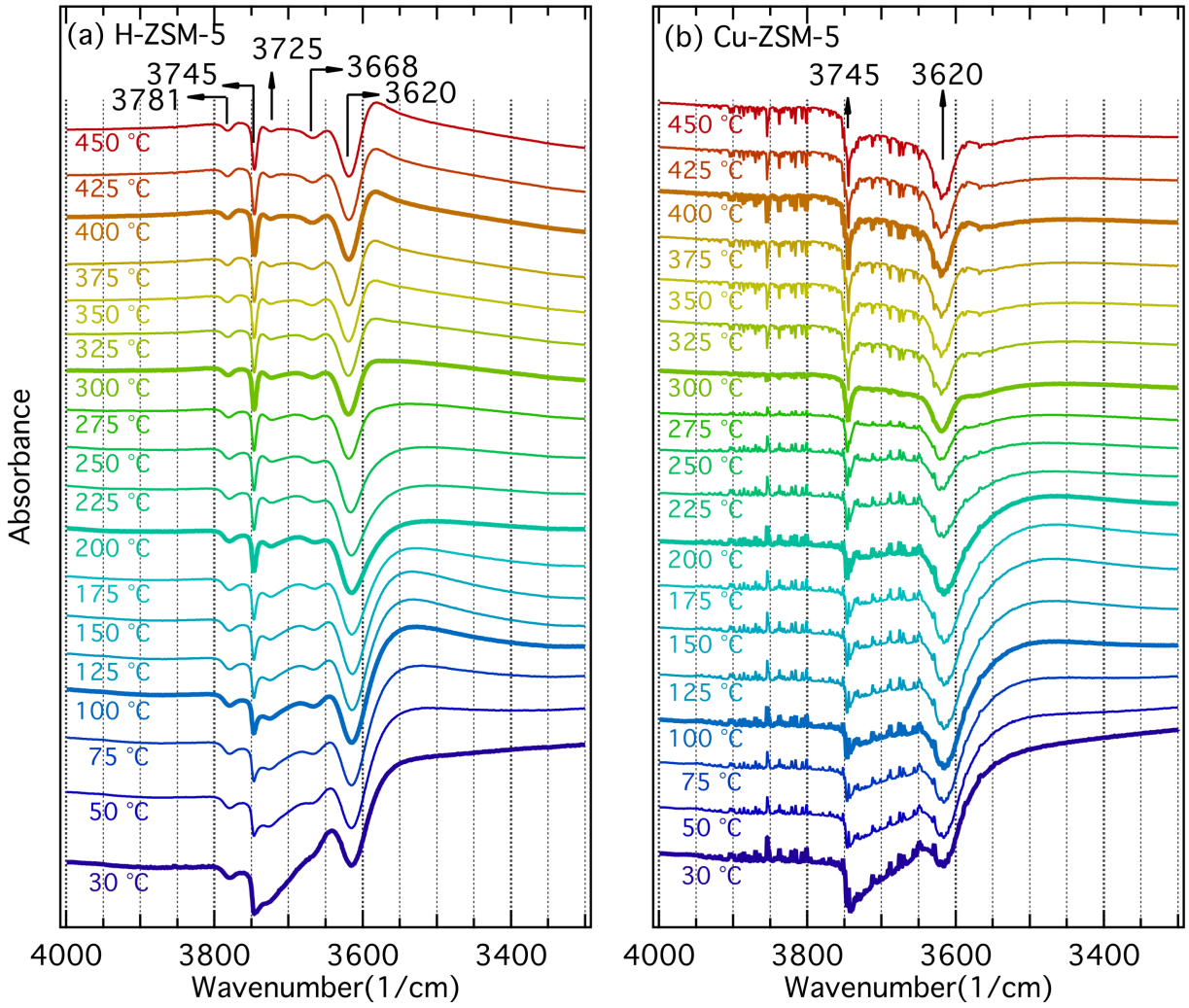

Figure 3: Series of selected DRIFT spectra of the O-H stretching region collected during methanol-TPD from 30 to 450 °C in Ar. The spectra are collected from (a) H-ZSM-5 and (b) Cu-ZSM-5.

negative peaks at 3745 and around 3620 cm^{-1} appear in both sets of spectra. The band at 3745 cm^{-1} is assigned to O-H stretching vibrations of terminal silanol groups and is denoted with $\nu[Si-OH]_{iso}$.[39–43] The somewhat broader band at 3620 cm^{-1} is associated with bridge-bonded OH species on Brønsted acid sites and here denoted with $\nu[Si-O(H)-Al]$.[41–43,49] The broadness of the latter band is possibly due to different Al positions in the ZSM-5 framework, resulting in OH species with different vibrational characteristics.

Additionally there are three minor bands at 3781, 3725 and 3668 cm^{-1}, which are more pronounced for the parent zeolite H-ZSM-5 (Figure 3a) than for the Cu-ZSM-5 sample (Figure 3b). The bands at 3725 and 3668 cm^{-1} can be assigned to O-H stretching vibrations of silanol groups associated with internal defects ($\nu[Si_{def}-OH]_{iso}$)[40,43] in the zeolite structure and O-H stretching vibrations of hydroxyl groups on extra framework Al ($\nu[Al_{ex}-OH]_{iso}$),[42,49] respectively. A reasonable explanation for the $\nu[Si_{def}-OH]_{iso}$ and $\nu[Al_{ex}-OH]_{iso}$ bands to be less intensive for the Cu-ZSM-5 sample is that during sample preparation, the framework defects constitute favourable Cu ion-exchange sites, such that fewer defect sites are available for hydroxyl groups after Cu functionalization. The band at 3781 cm^{-1}, however, has not yet been commonly observed or discussed in studies of ZSM-5. By comparing our IR spectra with IR studies of zeolite beta,[44,46–48] we assign this band to O-H stretching vibrations of isolated hydroxyl groups on isolated framework Al ($\nu[Al_{fr}-OH]_{iso}$). Methanol adsorbed on these Al sites perturbs the stretching vibrations of the attached hydroxyl groups, resulting in a negative peak at 3781 cm^{-1}. The absence of this band for the Cu-ZSM-5 sample can be due to lack of isolated hydroxyl groups on isolated framework Al before methanol adsorption, as a result of substitution of Cu ions to protons on the Brønsted acid sites.

After methanol adsorption, C-H stretching vibration bands around 3002, 2955, 2849 and 2780 cm^{-1} appear in the spectra for both samples at lower temperature, *i.e.* below 225 °C for Cu-ZSM-5 and below 200 °C for H-ZSM-5, as shown in Figure 4. The bands at 3002, 2955 and 2849 cm^{-1} are associated with hydrogen-bonded CH_3OH at lower temperature ($\nu[CH_3OH(liq)]$).[44,45] Heating the samples stepwise initially results in blue shift

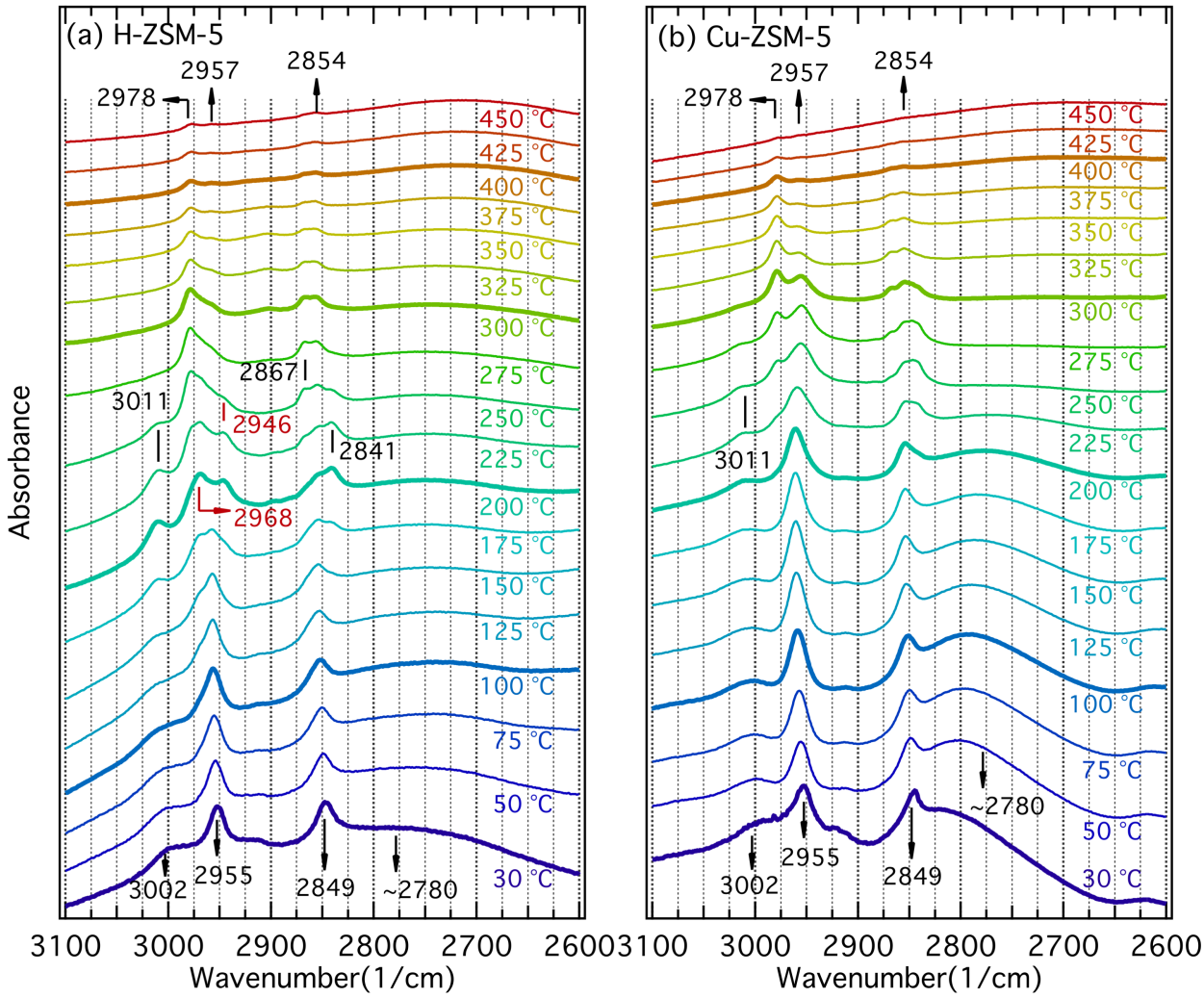

Figure 4: Series of selected DRIFT spectra of the C-H stretching region collected during methanol-TPD from 30 to 450 °C in Ar. The spectra are collected from (a) H-ZSM-5 and (b) Cu-ZSM-5.

of the absorption bands in the C-H stretching region, *i.e.* from 2955 and 2849 cm^{-1} to 2957 and 2854 cm^{-1}, respectively. According to previous studies, the bands at 2957 and 2854 cm^{-1} can be related to asymmetric ($\nu_{as}[Si_{ex} - OCH_3]$) and symmetric ($\nu_s[Si_{ex} - OCH_3]$) C-H stretching vibrations from methoxy groups adsorbed on extra framework Si, respectively.[40,44] Therefore, shift of the bands indicates desorption of liquid-like methanol, leaving the species, i.e. methoxy groups, interacting more strongly with the samples. At temperature below 125 °C, however, this band shift phenomenon can also be due to the decrease of methanol coverage with increased temperature. The assignments of the C-H stretching vibrations are reasonable also from a theoretical point of view. The calculated CH vibrational frequencies for methanol and methoxy groups (*i.e.* $\nu[Cu^+ - O(H)(CH_3)]$, $\nu[Cu^+ - OCH_3]$, $\nu[Cu^{2+} - OCH_3]$, $\nu[Cu^+ - O(H)(CH_3) - Cu^+]$ and $\nu[Cu^+ - O(CH_3) - Cu^+]$) fall broadly in the region 2693-3148 cm^{-1}. At the lower end of this region, however, the experimental observation is a rather broad band centered at around 2780 cm^{-1} whereas the peak shape of CH stretching vibrational features is expected to be sharp. Thus, for both samples, this band is assigned to the A band of the (A, B, C) triplet from zeolitic OH groups formed after methanol adsorption.[51,53,54] The characteristic (A, B, C) triplet, commonly observed around 2800, 2400 and 1700 cm^{-1} [51,53,54] appears after adsorption of methanol and is associated with methanol interactions via hydrogen bonds with the Brønsted acid sites.[51] Consequently, these three bands appear to be due to the Fermi resonance of zeolithic O-H stretching vibrations and overtones of zeolithic O-H bending vibrations of perturbed OH groups.[51] As shown in Figure S7, the (A, B, C) triplet appears after methanol adsorption and decreases in intensity simultaneously with increased temperature.

With increasing temperature, the bands in the C-H stretching region start to alter. These changes are accompanied with the intensity decrease of the (A, B, C) triplet, as shown in Figure S7. For the Cu-ZSM-5 sample (Figure 5b), the band at 2957 cm^{-1} splits into two peaks with maxima at 2978 and 2957 cm^{-1}. These two peaks can be associated with asymmetric C-H stretching vibrations of methoxy groups on Brønsted acid sites ($\nu_{as}[Si - O(CH_3) - Al]$)[39,40,45]

and on silicon ($\nu_{as}[\mathrm{Si_{ex}} - \mathrm{OCH_3}]$), respectively.[40,44] For the H-ZSM-5 sample, these two bands are evident although not discrete from each other. Additionally, two distinct absorption bands at 2968 and 2946 $\mathrm{cm^{-1}}$ appear only in the spectra for the H-ZSM-5 sample at moderate temperatures *i.e.* between 175 and 225 °C. These two bands have been assigned to methoxy groups adsorbed on extra lattice Al ($\nu_{as}[\mathrm{Al_{ex}} - \mathrm{OCH_3}]$)[44] and dimethyl ether (DME) that is hydrogen-bonded to Brønsted acid sites ($\nu[\mathrm{BAS} - \mathrm{O(CH_3)_2}]$),[45] respectively. The alternations of the bands around 2957 $\mathrm{cm^{-1}}$ indicate that with increasing temperature, the originally weakly adsorbed methanol is dehydrated or coupled such that methoxy groups and DME are formed on different sites in the zeolite framework. The absence of the $\nu_{as}[\mathrm{Al_{ex}} - \mathrm{OCH_3}]$ and $\nu[\mathrm{BAS} - \mathrm{O(CH_3)_2}]$ bands in the spectra for Cu-ZSM-5, however, can be due to inaccessibility of extra framework Al and some Brønsted acid sites as results from the Cu ion-exchange. This agrees with the observations of the absent $\nu[\mathrm{Si_{def}} - \mathrm{OH}]_{\mathrm{iso}}$ and $\nu[\mathrm{Al_{ex}} - \mathrm{OH}]_{\mathrm{iso}}$ bands in the O-H stretching region in the spectra of the Cu-ZSM-5 sample (Figure 3b). The presence of the $\nu_{as}[\mathrm{Si} - \mathrm{O(CH_3)} - \mathrm{Al}]$ and $\nu_{as}[\mathrm{Si_{ex}} - \mathrm{OCH_3}]$ bands that remain at high temperatures indicates that the Brønsted acid sites and extra framework Si possess the strongest interaction with the methoxy groups in the zeolite.

The group of absorption bands around 2856 $\mathrm{cm^{-1}}$, on the other hand, consists of three C-H stretching peaks at higher temperatures, *i.e.* above 175 °C for H-ZSM-5 and 225 °C for Cu-ZSM-5, with maxima at 2867, 2854 and 2841 $\mathrm{cm^{-1}}$. These bands are related to C-H stretching vibrations from methoxy groups on Brønsted acid sites ($\nu_s[\mathrm{Si} - \mathrm{O(CH_3)} - \mathrm{Al})]$),[45] methanol or methoxy groups on extra framework Si ($\nu_s[\mathrm{Si_{ex}} - \mathrm{OCH_3}]$)[40] and methanol adsorption on Brønsted acid sites ($\nu[\mathrm{BAS} - \mathrm{O(H)(CH_3)}]$),[50] respectively. For both sets of desorption spectra, the $\nu_s[\mathrm{Si_{ex}} - \mathrm{OCH_3}]$ band at 2854 $\mathrm{cm^{-1}}$ remains but with decreasing intensity with increasing temperature. The $\nu_s[\mathrm{Si} - \mathrm{O(CH_3)} - \mathrm{Al})]$ band appears at first and then decreases in intensity with increasing temperature, while the $\nu[\mathrm{BAS} - \mathrm{O(H)(CH_3)}]$ band only appears at moderate temperatures. The alternation of the bands around 2856 $\mathrm{cm^{-1}}$ indicates dehydration of weakly bonded methanol to methoxy groups as the temperature is increased.

Additionally, the pairs of bands at 2978/2867 cm^{-1} and 2957/2854 cm^{-1} are associated with asymmetric/symmetric C-H stretching vibrations of methoxy groups bonded to Brønsted acid sites and extra framework Si in ZSM-5. Only these two pairs of bands remain at high temperature, which indicates that the strongest forms of interaction during methanol-TPD is methoxy groups adsorbed on Brønsted acid sites or extra framework Si.

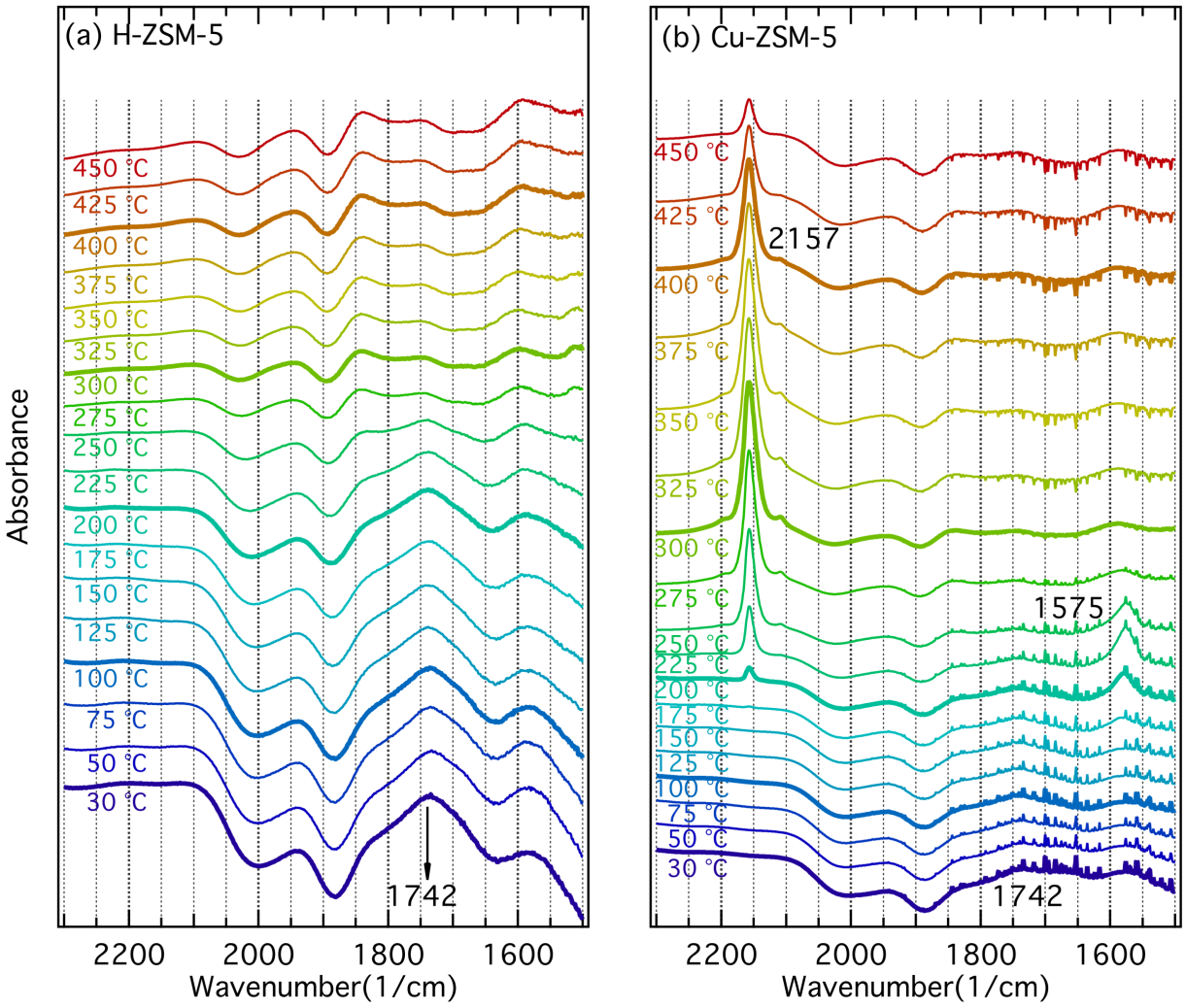

Figure 5: Series of selected DRIFT spectra of the C=O stretching/O-H bending region collected during methanol-TPD from 30 to 450 °C in Ar. The spectra are collected from (a) H-ZSM-5 and (b) Cu-ZSM-5.

In the C=O stretching/O-H bending region, an absorption band at 1742 cm^{-1} appears in the spectra for both Cu-ZSM-5 (Figure 5b) and H-ZSM-5 (Figure 5a) after methanol adsorp-

tion. This band can be assigned to the "C band" in the (A, B, C) triplet from vibrations of methanol perturbed zeolitic OH groups.[51,53,54] The intensity of the band at 1742 cm^{-1} decreases with increasing temperature, indicating dehydration of the zeolite. Simultaneously, two sharp bands rise at 2157 and 1575 cm^{-1} for Cu-ZSM-5 but not for the H-ZSM-5 sample. These bands are related to C=O stretching vibrations from CO formed on Cu species ($\nu[Cu^+ - CO]$) and formate ($\nu[Cu^+ - OCHO]$), respectively,[39,40,57] which can also be supported by the DFT calculation results in Table 1 (2124 and 1614 cm^{-1}). This is a strong indication of further oxidation of the adsorbed methanol related species proceeding on the Cu sites at higher temperature. To obtain high methanol selectivity for the partial oxidation of methane, the oxidation of methoxy groups should be avoided. The presented results suggest that the reaction temperature should be kept below 200 °C. One should, however, keep in mind that in those experiments the amount of methanol in the zeolite is likely higher than in a realistic case of stoichiometric or catalytic methanol formation. Hence, slightly higher reaction temperatures, say around 250 °C, may be acceptable.

The IR spectra taken during methanol-TPD reflect the dynamic interaction between methanol and Cu-ZSM-5. The entire methanol-TPD process can be summarized as follows: upon introduction of methanol, weak interactions between H-ZSM-5 and methanol are formed, resulting in methanol related C-H stretching bands at 3002, 2955, 2849 cm^{-1} as well as perturbed zeolitic O-H vibrations at ∼2780 and 1742 cm^{-1}. Methanol is the dominant adsorbed species on the defects in the zeolite framework structure and acidic sites in H-ZSM-5. The hydroxyl groups originally attached to these sites interact with methanol resulting in a decreased intensity of the absorption bands for these hydroxyl groups, *i.e.* 3781, 3745, 3668 and 3620 cm^{-1}. For Cu-ZSM-5, however, some of the protons in hydroxyl groups at zeolitic defects and the Brønsted acid sites are replaced with Cu ions during the ion-exchange. This results in a lack of hydroxyl groups on some of the defect sites such as internal silanols, extra framework Al as well as the distorted framework Al in Cu-ZSM-5 before methanol adsorption. Therefore, only changes of the remaining hydroxyl groups at

terminal silanol groups and Brønsted acid sites can be observed at 3745 and 3620 cm^{-1} after methanol adsorption. Additionally, dehydration of methanol takes place directly after methanol adsorption forming water on Cu-ZSM-5, which generates the water deformation band at 1647 cm^{-1}. The absence of the δ[HOH] band in the spectra of the H-ZSM-5 sample suggests that low-temperature dehydration of methanol takes place on the Cu sites. With increasing temperature, the liquid-like methanol desorbs while the species exhibiting stronger interactions remain adsorbed.This is presented in Figure S7, as changes in the C-H stretching region accompanied with intensity decrease of the (A, B, C) triplet. At 150 °C, methoxy groups become observable on extra framework Al sites in H-ZSM-5 (Figure 4a, band at 2968 cm^{-1}) followed by DME formation over the Brønsted acid sites at 200 °C (Figure 4a, bands at 2946 cm^{-1} and 3011 cm^{-1}). Whereas for Cu-ZSM-5, due to Cu ions on the ion-exchange sites, these bands are less pronounced. Formation of formate and CO (Figure 5b, bands at 1575 and 2157 cm^{-1}), however, is evident for Cu-ZSM-5 only, suggesting further oxidation of methanol and methoxy groups on Cu sites. At temperature above 300 °C, methoxy groups bound on Brønsted acid sites and extra framework Si become prominent represented by pairs of absorption bands at 2978/2867 cm^{-1} and 2957/2854 cm^{-1} in Figure 4 due to symmetric/asymmetric C-H stretching vibrations. These bands remain with reduced intensity at 450 °C indicating that methoxy groups bind strongly to the ZSM-5 framework.

Methanol-TPD experiments were also carried out under an oxidizing environment, *i.e.* 2 % O_2 balanced with Ar, for the Cu-ZSM-5 sample and its parent zeolite H-ZSM-5. Even though the spectra of each sample taken in O_2/Ar are rather similar to their corresponding spectra recorded during methanol-TPD in pure Ar, minor variations are observed for the Cu-ZSM-5 sample. Figure 6 presents the part of the spectra that are different from the ones taken in pure Ar. In particular, Figure 6 shows spectra taken from Cu-ZSM-5 during methanol-TPD from 30 to 450 °C in O_2/Ar for (a) the C-H stretching region (3100-2600 cm^{-1}) and (b) the C=O stretching/O-H bending region (2300-1500 cm^{-1}).

As shown in Figure 6a, in the C-H stretching region, additional to the absorption bands

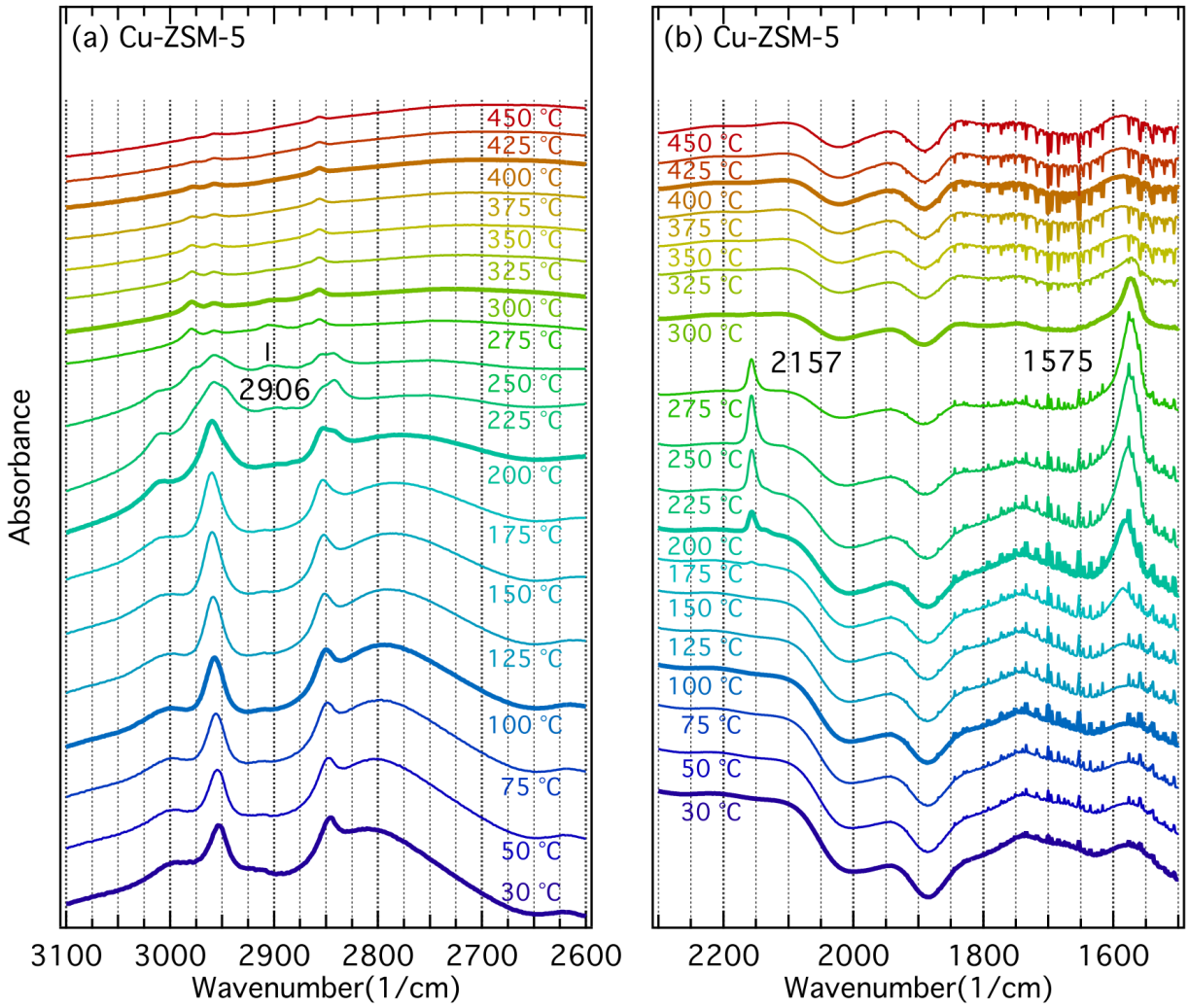

Figure 6: Series of selected DRIFT spectra collected from Cu-ZSM-5 during methanol-TPD from 30 to 450 °C in 2 % O_2 in Ar for (a) the C-H stretching region (3100-2600 cm^{-1}) and (b) the C=O stretching/O-H bending region (2300-1500 cm^{-1}).

observed in (Figure 4b), a band at 2906 cm^{-1} arises at temperatures between 225 and 275 °C. The appearance of this band is accompanied with high intensity of the $\nu[Cu^+ - OCHO]$ band at 1575 cm^{-1} in the C=O stretching region (Figure 5b). Therefore, the band at 2906 cm^{-1} can be associated with C-H stretching vibrations of adsorbed formate ($\nu[Cu^+ - OCHO]$). The absence of this band at temperatures where the $\nu[Cu^+ - OCHO]$ band is evident in the C=O stretching region can be due to the low amount of adsorbed formate, resulting in weak C-H stretching vibrations. For each temperature, the ratio between the $\nu[Cu^+ - OCHO]$ and $\nu[Cu^+ - CO]$ band intensities is considerably higher for spectra taken in O_2/Ar (Figure 6b) than for spectra recorded in Ar alone (Figure 5b). This result is likely connected to higher concentrations of framework oxygen when oxygen is present in the gas phase.

In summary, our spectroscopic results show that formed methoxy species, as an important reaction intermediate, are stable in Cu-ZSM-5. On one hand, the stability of the methoxy species may play an important role in preventing further oxidation to unwanted products during partial oxidation of methane to methanol. On the other hand, the high methoxy stability is likely the reason for the necessary extraction step in the sequential Activation-Reaction-Extraction process. In this view, tuning of the catalyst-methoxy interaction properties is one of the important design principles for improving catalyst formulations for direct partial oxidation of methane to methanol. Preferable, a good catalyst should possess oxygen species that can break the CH bond in methane, while the oxygen metal bond strength should be moderate to facilitate conversion of methoxy species to methanol. Generally, in selective oxidation, tuning the metal-oxygen bond strength is one of the important design principles.[58] Though the goal is clear, the approach whereby this can be achieved is not straightforward. Many studies suggest that Cu dimers and/or trimers constitute the main active site(s). Accepting this view, one would like to modify/promote the active site possibly by the support or directly by creating active centers consisting of Cu ions interacting with other (ionic) elements that collectively form more active dimers and/or trimers.

Conclusion

This work presents an *in situ* infrared spectroscopic study of methanol desorption for Cu-ZSM-5 at temperatures from 30 to 450 °C with support from first-principles calculations. By following the dynamic interaction between methanol and Cu-ZSM-5, we conclude that: i) the Brønsted acid sites and defects in the framework structure of the zeolite, *i.e.* extra framework Al and extra framework Si, constitute ion-exchange sites for Cu ions; ii) the Cu species in Cu-ZSM-5 are responsible for interaction with methanol that is additional to the methanol adsorbed on the ZSM-5 framework; iii) the Cu species in Cu-ZSM-5 are responsible for further oxidation of methanol and methoxy groups to formate and CO; iv) strong interactions are observed between methoxy groups and zeolitic framework sites, *i.e.* the Brønsted acid sites and extra framework Si, suggesting the necessity of the proton extraction step during direct partial oxidation of methane to methanol over Cu-ZSM-5.

Supporting information

Parameters from curve fitting analysis of the EXAFS spectra on the Cu-ZSM-5 24h sample; IR spectra of the Cu-ZSM-5 24h sample during methanol-TPD; TEM characterization on the Cu-ZSM-5 24h sample; XRD and IR spectra during methanol-TPD on the Cu-ZSM-5 6h sample; Motifs used in the DFT calculations.

Acknowledgement

The authors thank MAX IV Laboratory (Lund, Sweden) for providing the beamtimes. The computations were performed on resources provided by the Swedish National Infrastructure for Computing (SNIC) at C3SE. This work is financially supported by the Swedish Research Council through the Röntgen-Ångström collaborations "Catalysis on the atomic scale" (No. 349-2011-6491) and "Time-resolved in situ methods for design of catalytic sites within sus-

tainable chemistry" (No. 349-2013-567), the Knut and Alice Wallenberg foundation [No. 2015.0058], as well as the Competence Centre for Catalysis, which is financially supported by Chalmers University of Technology, the Swedish Energy Agency and the member companies: AB Volvo, ECAPS AB, Haldor Topsøe A/S, Volvo Car Corporation AB, Scania CV AB, and Wärtsilä Finland Oy.

References

(1) da Silva, M. J. Synthesis of Methanol from Methane: Challenges and Advances on the Multi-Step (Syngas) and One-Step Routes (DMTM). *Fuel Process. Technol.* **2016**, *145*, 42–61.

(2) Citek, C.; Gary, J. B.; Wasinger, E. C.; Stack, T. D. Chemical Plausibility of Cu(III) with Biological Ligation in pMMO. *J. Am. Chem. Soc.* **2015**, *137*, 6991–4.

(3) Nordlund, P.; Dalton, H.; Eklund, H. The Active Site Structure of Methane Monooxygenase is Closely Related to the Binuclear Iron Center of Ribonucleotide Reductase. *FEBS Lett.* **1992**, *307*, 257–262.

(4) Balasubramanian, R.; Smith, S. M.; Rawat, S.; Yatsunyk, L. A.; Stemmler, T. L.; Rosenzweig, A. C. Oxidation of Methane by a Biological Dicopper Centre. *Nature* **2010**, *465*, 115–U131.

(5) Groothaert, M. H.; Smeets, P. J.; Sels, B. F.; Jacobs, P. A.; Schoonheydt,; A., R. Selective Oxidation of Methane by the Bis(μ-oxo)dicopper Core Stabilized on ZSM-5 and Mordenite Zeolites. *J. Am. Chem. Soc.* **2005**, *127*, 1394–1395.

(6) Yumura, T.; Takeuchi, M.; Kobayashi, H.; Kuroda, Y. Effects of ZSM-5 Zeolite Confinement on Reaction Intermediates during Dioxygen Activation by Enclosed Dicopper Cations. *Inorg. Chem.* **2009**, *48*, 508–517.

(7) Woertink, J. S.; Smeets, P. J.; Groothaert, M. H.; Vance, M. A.; Sels, B. F.; Schoonheydt, R. A.; Solomon, E. I. A $[Cu_2O]^{2+}$ Core in Cu-ZSM-5, the Active Site in the Oxidation of Methane to Methanol. *Proc. Natl. Acad. Sci. U. S. A.* **2009**, *106*, 18908–18913.

(8) Smeets, P. J.; Groothaert, M. H.; Schoonheydt, R. A. Cu Based Zeolites: A UV-Vis Study of the Active Site in the Selective Methane Oxidation at Low Temperatures. *Catal. Today* **2005**, *110*, 303–309.

(9) Beznis, N. V.; Weckhuysen, B. M.; Bitter, J. H. Cu-ZSM-5 Zeolites for the Formation of Methanol from Methane and Oxygen: Probing the Active Sites and Spectator Species. *Catal. Lett.* **2010**, *138*, 14–22.

(10) Sheppard, T.; Hamill, C. D.; Goguet, A.; Rooney, D. W.; Thompson, J. M. A Low Temperature, Isothermal Gas-Phase System for Conversion of Methane to Methanol over Cu-ZSM-5. *Chem. Commun. (Cambridge, U. K.)* **2014**, *50*, 11053–5.

(11) Smeets, P. J.; Hadt, R. G.; Woertink, J. S.; Vanelderen, P.; Schoonheydt, R. A.; Sels, B. F.; Solomon, E. I. Oxygen Precursor to the Reactive Intermediate in Methanol Synthesis by Cu-ZSM-5. *J. Am. Chem. Soc.* **2010**, *132*, 14736–14738.

(12) Sainz-Vidal, A.; Balmaseda, J.; Lartundo-Rojas, L.; Reguera, E. Preparation of Cu-mordenite by Ionic Exchange Reaction Under Milling: A Favorable Route to Form the Mono-(μ-oxo) Dicopper Active Species. *Microporous Mesoporous Mater.* **2014**, *185*, 113–120.

(13) Narsimhan, K.; Iyoki, K.; Dinh, K.; Román-Leshkov, Y. Catalytic Oxidation of Methane into Methanol over Copper-Exchanged Zeolites with Oxygen at Low Temperature. *ACS Cent. Sci.* **2016**, *2*, 424–9.

(14) Grundner, S.; Markovits, M. A. C.; Li, G.; Tromp, M.; Pidko, E. A.; Hensen, E. J. M.; Jentys, A.; Sanchez-Sanchez, M.; Lercher, J. A. Single-Site Trinuclear Copper Oxygen

Clusters in Mordenite for Selective Conversion of Methane to Methanol. *Nat. Commun.* **2015**, *6*, 7546.

(15) Vanelderen, P.; Hadt, R. G.; Smeets, P. J.; Solomon, E. I.; Schoonheydt, R. A.; Sels, B. F. Cu-ZSM-5: A Biomimetic Inorganic Model for Methane Oxidation. *J. Catal.* **2011**, *284*, 157–164.

(16) Narsimhan, K.; Michaelis, V. K.; Mathies, G.; Gunther, W. R.; Griffin, R. G.; Román-Leshkov, Y. Methane to Acetic Acid over Cu-Exchanged Zeolites: Mechanistic Insights from a Site-Specific Carbonylation Reaction. *J. Am. Chem. Soc.* **2015**, *137*, 1825–1832.

(17) Tang, P.; Zhu, Q.; Wu, Z.; Ma, D. Methane Activation: the Past and Future. *Energy Environ. Sci.* **2014**, *7*, 2580.

(18) Kulkarni, A. R.; Zhao, Z.-J.; Siahrostami, S.; Nørskov, J. K.; Studt, F. Monocopper Active Site for Partial Methane Oxidation in Cu-Exchanged 8MR Zeolites. *ACS Catal.* **2016**, 6531–6536.

(19) Li, G.; Vassilev, P.; Sanchez-Sanchez, M.; Lercher, J. A.; Hensen, E. J. M.; Pidko, E. A. Stability and Reactivity of Copper Oxo-Clusters in ZSM-5 Zeolite for Selective Methane Oxidation to Methanol. *J. Catal.* **2016**, *338*, 305–312.

(20) Smeets, P. J.; Woertink, J. S.; Sels, B. F.; Solomon, E. I.; Schoonheydt,; A., R. Transition-Metal Ions in Zeolites: Coordination and Activation of Oxygen. *Inorg. Chem.* **2010**, *49*, 3573–3583.

(21) Ravel, B.; Newville, M. ATHENA, ARTEMIS, HEPHAESTUS: Data Analysis for X-ray Absorption Spectroscopy Using IFEFFIT. *J. Synchrotron Radiat.* **2005**, *12*, 537–541.

(22) Wan, W.; Hovmöller, S.; Zou, X. Structure Projection Reconstruction from Through-Focus Series of High-Resolution Transmission Electron Microscopy Images. *Ultramicroscopy* **2012**, *115*, 50–60.

(23) Kresse, G.; Furthmüller, J. Efficiency of Ab-Initio Total Energy Calculations for Metals and Semiconductors Using a Plane-Wave Basis Set. *Comput. Mater. Sci.* **1996**, *6*, 15–50.

(24) Kresse, G.; Furthmüller, J. Efficient Iterative Schemes for Ab Initio Total-Energy Calculations Using a Plane-Wave Basis Set. *Phys. Rev. B* **1996**, *54*, 11169–11186.

(25) Blöchl, P. E. Projector Augmented-Wave Method. *Phys. Rev. B* **1994**, *50*, 17953–17979.

(26) Klimeš, J.; Bowler, D. R.; Michaelides, A. Van Der Waals Density Functionals Applied to Solids. *Phys. Rev. B* **2011**, *83*, 195131.

(27) Perdew, J. P.; Burke, K.; Ernzerhof, M. Generalized Gradient Approximation Made Simple. *Phys. Rev. Lett.* **1996**, *77*, 3865–3868.

(28) Tsai, M.-L.; Hadt, R. G.; Vanelderen, P.; Sels, B. F.; Schoonheydt, R. A.; Solomon, E. I. $[Cu_2O]^{2+}$ Active Site Formation in Cu-ZSM-5: Geometric and Electronic Structure Requirements for N_2O Activation. *J. Am. Chem. Soc.* **2014**, *136*, 3522–3529.

(29) Arvidsson, A. A.; Zhdanov, V. P.; Carlsson, P.-A.; Grönbeck, H.; Hellman, A. Metal Dimer Sites in ZSM-5 Zeolite for Methane-to-Methanol Conversion from First-Principles Kinetic Modelling: Is the $[Cu–O–Cu]^{2+}$ Motif Relevant for Ni, Co, Fe, Ag, and Au? *Catal. Sci. Technol.* **2017**, *7*, 1470–1477.

(30) van Koningsveld, H.; van Bekkum, H.; Jansen, J. C. On the Location and Disorder of the Tetrapropylammonium (TPA) Ion in Zeolite ZSM-5 with Improved Framework Accuracy. *Acta Crystallogr., Sect. B: Struct. Sci.* **1987**, *43*, 127–132.

(31) Bahn, S. R.; Jacobsen, K. W. An Object-Oriented Scripting Interface to a Legacy Electronic Structure Code. *Comput. Sci. Eng.* **2002**, *4*, 56–66.

(32) Inorganic Crystal Structure Database. `https://icsd.fiz-karlsruhe.de/`, (accessed Feburary, 2017).

(33) Mlekodaj, K.; Tarach, K.; Datka, J.; Góra-Marek, K.; Makowski, W. Porosity and Accessibility of Acid Sites in Desilicated ZSM-5 Zeolites Studied Using Adsorption of Probe Molecules. *Microporous Mesoporous Mater.* **2014**, *183*, 54–61.

(34) Hudec, P.; Smieskova, A.; Zidek, Z.; Zubek, M.; Schneider, P.; Kocirk, M.; Kozankova, J. Adsorption Properties of ZSM-5 Zeolites. *Collect. Czech. Chem. Commun.* **1997**, *63*, 141–154.

(35) Thommes, M.; Kaneko, K.; Neimark, A. V.; Olivier, J. P.; Rodriguez-Reinoso, F.; Rouquerol, J.; Sing, K. S. W. Physisorption of Gases, with Special Reference to the Evaluation of Surface Area and Pore Size Distribution (IUPAC Technical Report). *Pure Appl. Chem.* **2015**, *87*, 1051–1069.

(36) Lamberti, C.; Bordiga, S.; Salvalaggio, M.; Spoto, G.; Zecchina, A.; Geobaldo, F.; Vlaic, G.; Bellatreccia, M. XAFS, IR, and UV-Vis Study of the Cu^{I} Environment in Cu^{I}-ZSM-5. *J. Phys. Chem. B* **1997**, *101*, 344–360.

(37) Groothaert, M. H.; Bokhoven, v. J. A.; Battiston, A. A.; Weckhuysen, B. M.; Schoonheydt, R. A. Bis(μ-oxo)dicopper in Cu-ZSM-5 and Its Role in the Decomposition of NO: A Combined *in Situ* XAFS, UV-Vis-Near-IR, and Kinetic Study. *J. Am. Chem. Soc.* **2002**, *125*, 7629–7640.

(38) The Farrel Lytle database. `http://ixs.csrri.iit.edu/database/data/Farrel_Lytle_data/`, (accessed May, 2017).

(39) Kung, M. C.; Lin, S. S. Y.; Kung, H. H. *In situ* Infrared Spectroscopic Study of CH_4 Oxidation Over Co-ZSM-5. *Top. Catal.* **2012**, *55*, 108–115.

(40) Wood, B. R.; Reimer, J. A.; Bell, A. T.; Janicke, M. T.; Ott, K. C. Methanol Formation on Fe/Al-MFI via the Oxidation of Methane by Nitrous Oxide. *J. Catal.* **2004**, *225*, 300–306.

(41) Sárkány, J. Zeolite Proton-Assisted Reoxidation of CuO in Over-Exchanged Cu^{II}-ZSM-5 Reduced by Hydrogen. (1) Reoxidation in Ar stream: an FTIR Study. *Phys. Chem. Chem. Phys.* **1999**, *1*, 5251–5257.

(42) Ene, A. B.; Archipov, T.; Roduner, E. Spectroscopic Study of the Adsorption of Benzene on Cu/HZSM5 Zeolites. *J. Phys. Chem. C* **2010**, *114*, 14571–14578.

(43) Starokon, E. V.; Parfenov, M. V.; Arzumanov, S. S.; Pirutko, L. V.; Stepanov, A. G.; Panov, G. I. Oxidation of Methane to Methanol on the Surface of FeZSM-5 Zeolite. *J. Catal.* **2013**, *300*, 47–54.

(44) Nobukawa, T.; Yoshida, M.; Kameoka, S.; Ito, S.-i.; Tomishige, K.; Kunimori, K. *In-Situ* Observation of Reaction Intermediate in the Selective Catalytic Reduction of N_2O with CH_4 over Fe Ion-Exchanged BEA Zeolite Catalyst for the Elucidation of Its Reaction Mechanism Using FTIR. *J. Phys. Chem. B* **2004**, *108*, 4071–4079.

(45) Campbell, S. M.; Jiang, X.-Z.; Howe, R. F. Methanol to Hydrocarbons: Spectroscopic Studies and the Significance of Extra-Framework Aluminium. *Microporous Mesoporous Mater.* **1999**, *29*, 91–108.

(46) Bourgeat-Lami, E.; Massiani, P.; Renzo, F. D.; Espiau, P.; Fajula, F.; Courières, T. D. Study of the State of Aluminium in Zeolite-β. *Appl. Catal.* **1991**, *72*, 139–152.

(47) Kiricsi, I.; Flego, C.; Pazzuconi, G.; Parker, W. O.; Millini, R.; Perego, C.; Bellussi, G. Progress toward Understanding Zeolite-Beta Acidity: An IR and ^{27}Al NMR Spectroscopic Study. *J. Phys. Chem.* **1994**, *98*, 4627–4634.

(48) Vimont, A.; Thibault-Starzyk, F.; Lavalley, J. Infrared Spectroscopic Study of the Acidobasic Properties of Beta Zeolite. *J. Phys. Chem. B* **2000**, *104*, 286–291.

(49) Datka, J.; Gil, B.; Kawałek, M.; Staudte, B. Low Temperature IR Studies of CO Sorbed in ZSM-5 Zeolites. *J. Mol. Struct.* **1999**, *511-512*, 133–139.

(50) Zhang, Y.; Drake, I.; Briggs, D.; Bell, A. Synthesis of Dimethyl Carbonate and Dimethoxy Methane over Cu-ZSM-5. *J. Catal.* **2006**, *244*, 219–229.

(51) Haase, F.; Sauer, J. Interaction of Methanol with Brønsted Acid Sites of Zeolite Catalysts: An ab Initio Study. *J. Am. Chem. Soc.* **1995**, *117*, 3780–3789.

(52) Hadjiivanov, K. I.; Kantcheva, M. M.; Klissurski, D. G. IR Study of CO Adsorption on Cu-ZSM-5 and CuO/SiO_2 Catalysts: δ and π Components of the Cu^+-CO Bond. *J. Chem. Soc., Faraday Trans.* **1996**, *92*, 4595–4600.

(53) Pelmenschikov, A. G.; van Wolput, J. H. M. C.; Jänchen, J.; van Santed, R. A. (A,B,C) Triplet of Infrared OH Bands of Zeolitic H-Complexes. *J. Phys. Chem.* **1995**, *99*, 3612–3617.

(54) Pelmenschikov, A. G.; van Santen, R. A.; Jänchen, J.; Meijer, E. CD_3CN as a Probe of Lewis and Bronsted Acidity of Zeolites. *J. Phys. Chem.* **1993**, *97*, 11071–11074.

(55) Kwak, J. H.; Varga, T.; Peden, C. H. F.; Gao, F.; Hanson, J. C.; Szanyi, J. Following the Movement of Cu Ions in a SSZ-13 Zeolite During Dehydration, Reduction and Adsorption: A Combined *in situ* TP-XRD, XANES/DRIFTS Study. *J. Catal.* **2014**, *314*, 83–93.

(56) Crupi, V.; Longo, F.; Majolino, D.; Venuti, V. Vibrational Properties of Water Molecules Adsorbed in Different Zeolitic Frameworks. *J. Phys.: Condens. Matter* **2006**, *18*, 3563–3580.

(57) Engeldinger, J.; Domke, C.; Richter, M.; Bentrup, U. Elucidating the Role of Cu Species in the Oxidative Carbonylation of Methanol to Dimethyl Carbonate on CuY: An *in situ* Spectroscopic and Catalytic Study. *Appl. Catal., A* **2010**, *382*, 303–311.

(58) Grasselli, R. K. Fundamental Principles of Selective Heterogeneous Oxidation Catalysis. *Top. Catal.* **2002**, *21*, 79–88.

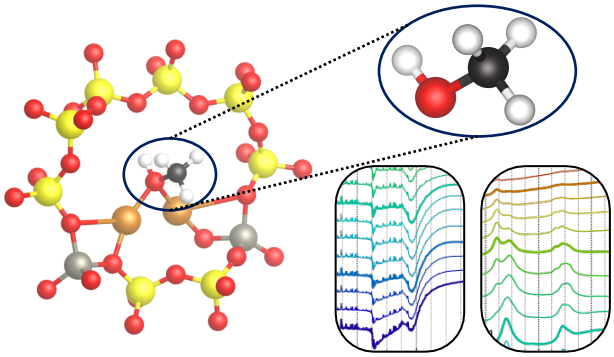

TOC Graphic